JTAE

E- ISSN: 2676-4253

Journal of Technology in Aerospace Engineering

Vol. 9, Special Issue, pp. 1-8, 2025

https://doi.org/10.22034/jtae.yyyy.nnnn

Journal Homepage: https://www.jtae.ari.ac.ir

Original Research Paper

Shock Reflection Behavior in High-Speed Rarefied Gas Flow

Arash Divazi and Hassan Akhlaghi*

College of Interdisciplinary Science and Technology, University of Tehran, Tehran, Iran

ARTICLE INFO

Article History:

Received 9 August 2025
Revised 12 October 2025
Accepted 1 November 2025
Available Online 1 November 2025

Keywords:

Rarefied gas flow
Direct simulation MONTE CARLO
Shockwave reflection
DSMC Foam
Continuum gas flow

ABSTRACT

The behavior of shock wave reflection under varying levels of flow rarefaction is investigated using the Direct Simulation Monte Carlo (DSMC) method. An internal supersonic flow of monoatomic Argon gas over a sudden ramp geometry is considered as the test case. The simulations are carried out with the dsmcFoam solver, a DSMC module of the OpenFOAM package. Initially, the shock reflection phenomenon in the continuum limit is verified through comparison with conventional Computational Fluid Dynamics (CFD) simulations based on the Navier–Stokes equations and with analytical predictions from gas dynamics theory. Following this validation, the influence of rarefaction is examined by progressively decreasing the upstream flow density to achieve different Knudsen number regimes. The results demonstrate that increased rarefaction leads to significant thickening of both the incident and reflected shock waves, with the effect being more pronounced for the reflected shock. Furthermore, the reflected shock exhibits stronger deviations from its continuum counterpart in terms of shape and sharpness. At the shock–ramp interaction points, where a straight shock profile is expected under continuum conditions, the simulations reveal the formation of a curved shock front. This curvature is attributed to the emergence of localized non-equilibrium flow regions, where the assumptions of local thermodynamic equilibrium no longer hold. These findings provide new insights into shock structure modification in rarefied gas flows, relevant to microscale devices and high-altitude hypersonic flight applications.

* Corresponding Author's E-mail: hassan.akhlaghi@ut.ac.ir

How to Cite this Article:
A. Divazi and H. Akhlaghi, "Shock reflection behavior in high-speed rarefied gas flow," *Journal of Technology in Aerospace Engineering*, Vol. 9, Special Issue, pp. 1-8, 2025, https://doi.org/10.22034/jtae.yyyy.nnnn.

NOMENCLATURE

P	Pressure
P0	Initial pressure
T	Temperature
T0	Initial temperature
X	X-Coordinate
f	Velocity distribution function (before collision)
f_1	Velocity distribution function (before collision, partner molecule)
f'	Velocity distribution function (after collision)
f_1'	Velocity distribution function (after collision, partner molecule)
n	Number density
r	Space vector
c	Velocity space vector
c_r	relative velocity between a molecule with velocity class c

Greek symbols

σdΩ	differential cross section for the collision of a molecule of class ***c***

1 INTRODUCTION

Shockwave reflection in rarefied gas flows is a complex phenomenon relevant in high-speed aerodynamics, hypersonic flows, and vacuum system design. The study focuses on the interaction of shockwaves with boundaries, flow fields, and reflected waves in low-density regimes where the continuum assumption breaks down. Rarefied flows are characterized by the Knudsen number (Kn), which measures the degree of rarefaction, necessitating computational and theoretical approaches like the Direct Simulation Monte Carlo (DSMC) method and Boltzmann equation-based models.

Bird [1] showed that in highly rarefied flows, shockwaves are not sharp discontinuities but have finite thickness due to reduced collisional effects. Nance and Hassan [2] extended these studies, examining shockwave interactions with surfaces and highlighting the influence of wall accommodation coefficients. Titarev *et al.* [3] explored the reflection of a uniform supersonic rarefied-gas flow incident on a wall with an orifice. Using the kinetic S-model, they examined the influence of the orifice on the reflection nature, the velocity of the reflected shock wave, and the formation of a gas jet flowing into a vacuum. Their findings highlighted the complex interactions between the shockwave and the orifice, which significantly affect the reflection characteristics. Akhlaghi et al. [4] studied shock polar behavior (θ-β, hodograph, θ-P) in supersonic rarefied flows over cylinders using DSMC (RGS2D solver), resulting in observed rarefaction-induced increases in shock angle, max flow deflection, and aft shock pressure, alongside decreased post-shock velocities, demonstrating Knudsen number dependence. Takata *et al.* [5] investigated the effects of rarefaction on shock reflections using molecular dynamics simulations. Their work revealed significant deviations in density and temperature profiles at shock boundaries, influencing reflection behavior. Holtz and Muntz [6] examined velocity distribution functions near shock boundaries, showing anisotropy in molecular velocities, which plays a critical role in shaping reflected shock characteristics. Zuppardi and Boffa [7] focused on shockwave interaction with walls in rarefied conditions, highlighting how surface roughness and thermal accommodation coefficients affect reflection patterns. Gardner and Agarwal [8] studied the influence of rarefaction on shock reflection over hypersonic forebodies, focusing on how it affects heat transfer and pressure distribution. Using a combination of DSMC method and modified Navier-Stokes equations, the study reveals that rarefaction significantly alters the thermal and pressure characteristics of the shock reflection process. Akhlaghi *et al.* [9] studied rarefied Couette flow modeling with a novel first-order velocity slip model and DSMC-derived wall-function viscosity, resulting in accurate nonlinear velocity profile predictions and demonstrating that rarefaction-aware viscosity models enable simpler slip models in Navier-Stokes simulations, improving accuracy for near-wall rarefied flows. Roohi et al. [10] studied airfoil aerodynamics in rarefied environments with a semi-analytical method and parametric studies, resulting in quantified effects of rarefaction, Mach number, Reynolds number, angle of attack, camber, and thickness on aerodynamic performance. Jiang *et al.* [11] investigated rarefied hypersonic shock-shock interaction using DSMC and demonstrated

that higher Knudsen numbers diminish the intensity and thermal load augmentation caused by the interaction.

In the current research, we investigate the shock reflection behavior for a supersonic inflow channel faced with a sudden ramp, for the Argon gas. Simulation results will be performed via DSMC method under dsmcFoam package. The effect of flow rarefaction on the incident and reflected shockwave patterns is examined. Also, the pressure and temperature distributions through the incident and reflected shockwaves are considered and discussed.

2 MATERIAL AND METHOD

2.1 Direct simulation Monte Carlo method

The Direct Simulation Monte Carlo (DSMC) method offers a computational solution to the Boltzmann equation by directly simulating molecular processes statistically [12]. Each particle in the simulation represents a large number of real gas molecules. The flowchart of this method is illustrated below in Figure 1. The computational approach begins with the Boltzmann equation, which serves as the foundation for describing molecular behavior. As defined in equation (1) from the paper, the Boltzmann equation tracks the evolution of the velocity distribution function, accounting for both molecular movements and collisions.

$$\frac{\partial}{\partial t}(nf) + c\frac{\partial}{\partial r}(nf) = \int_{-\infty}^{+\infty}\int_{0}^{4\pi} n^2\left(\acute{f}\acute{f}_1 - ff_1\right)c_r\sigma d\Omega dc \qquad (1)$$

2.2 dsmcFoam solver

dsmcFoam, a parallel DSMC solver, can model arbitrary geometries and multiple gas species on parallel computers. It employs various collision models, comparable to codes like MONACO and PDSC. The solver benefits from OpenFOAM's hierarchical structure, allowing users to utilize most features without extensive coding knowledge. Functions are categorized and shown in Figure 2. More details on its algorithms can be found in the referenced study.

In this study, dsmcFoam v12 has been utilized. For binary collision modeling, the Larsen Borgnakke Variable Hard Sphere (LB-VHS) model, along with Specular Reflection as the wall interaction model, have been employed. The constants of this model, including Tref and relaxation Collision Number, are 298.15 and 5.0 respectively. The Argon mass is 66.3e-27, diameter is 4.17e-10, internal Degrees Of Freedom is 0, and viscosity index (omega) is 0.81.

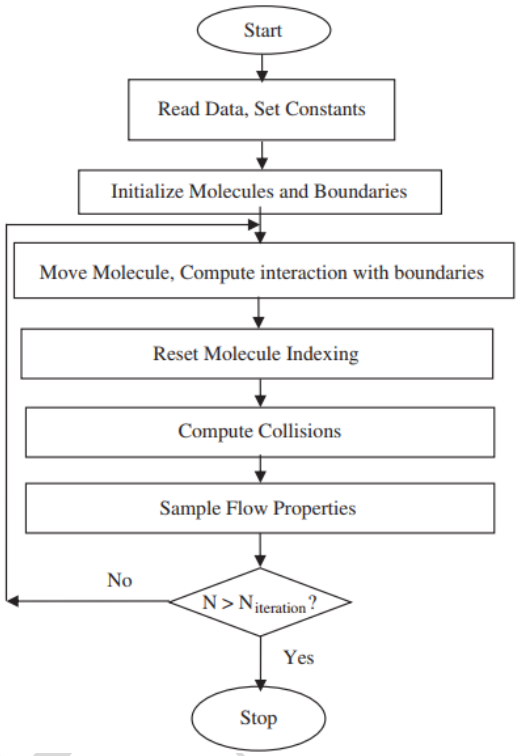

Fig. 1. Flowchart of the DSMC algorithm

2.3 Physical specifications

In this study, a converging channel is selected as the geometry. The channel has a length of 1.7 m, a height of 0.5m, and a width of 1m. Since the geometry is 2D, there is only 1 cell in the width of the channel. The boundary conditions for the CFD case are: velocity inlet at the left, pressure outlet at the right, symmetry at the top and forehead of the ramp at the bottom, and a wall with a turn angle of 10° at the ramp. The viscous model selected is Laminar with a density-based steady-state solver.

The inlet conditions are a velocity of 736.5 m/s at a temperature of 150K, forming a supersonic inlet at Mach 3.2 for Argon gas. In the DSMC, inlet and outlet have Free Stream boundary conditions. The pressure is considered to be 2 atm at the inlet of the near-continuum case.

After calculating the collision frequency, the time step for the DSMC solver is obtained to be 1.0×10^{-8} s. For the continuum limit case, the nEquivalent-Particles is equal to 1.515×10^{20}, and the Number Density is 9.79×10^{25}, resulting in an average of 20

particles per cell. For the near-continuum case, the density is reduced by 10^{-5} order. Therefore, the first case is named 1.0×10^{-5}. After this, the rarefaction of the rest of the cases increases step by step as 0.5×10^{-5}, 0.25×10^{-5}, 1.0×10^{-6}, 0.5×10^{-6}, 0.25×10^{-6}.

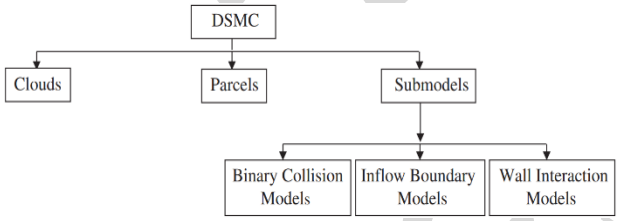

Fig. 2. Directory of dsmcFoam solver

3 SOLVER VERIFICATION

To verify the solver's reliability and capability in this case, a verification with the commercial solver Fluent 24.0, as well as analytical relations and results, has been conducted. The simulation grids used for both CFD and DSMC are shown in Figure 3, which contains 21,000 structured cells. It should be noted that adaptive mesh refinement has been applied to the CFD case to improve the precision of shock capturing. Since this study compares the results of shock reflection behavior from the continuum to the rarefied regime, and the NS equations are valid in the continuum regime, the verification has been carried out for a near-continuum regime.

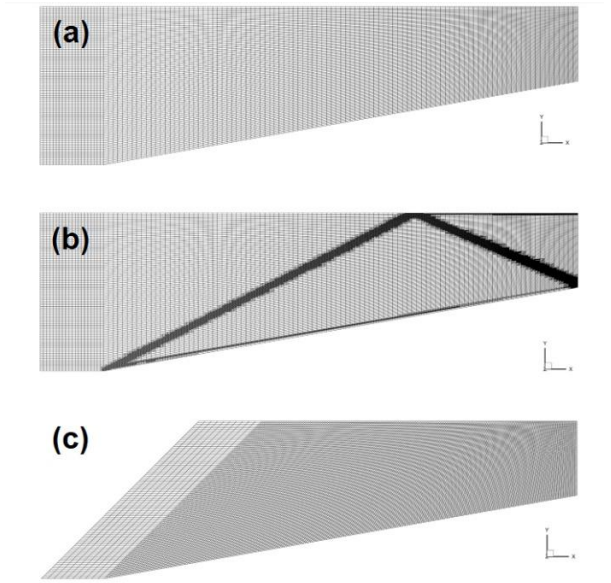

Fig. 3. Computational domain and employed grid for CFD (a-b) and DSMC (c) calculations

A comparison between Mach number contours can be seen in Figure 4 below, which shows an acceptable agreement among analytical, CFD, and DSMC solutions (wave angle of 27°). Additionally, the Mach numbers, reflection, and location of shock in the continuum (CFD) and near-continuum (DSMC) solutions show adequate and precise similarity.

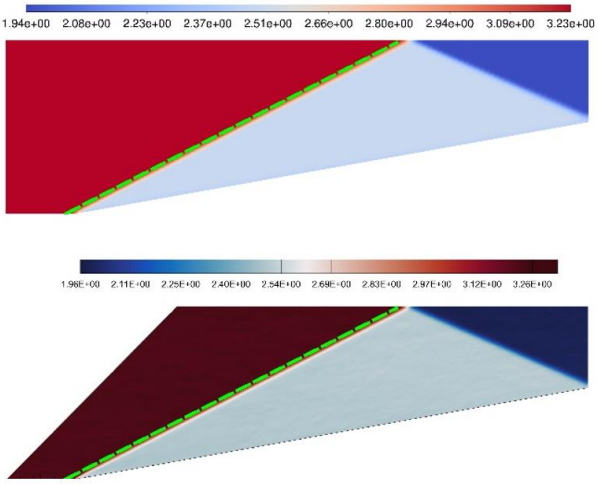

Fig. 4. Contours of Mach number obtained by CFD (upper) and DSMC (lower). The analytical solution is indicated by dashed lines.

Moreover, Figure 5 validates the DSMC near-continuum solution with CFD full continuum results. It compares the pressure ratio of both cases on a line crossing through both shockwave and its reflection from the inlet to outlet, at 50% distance from the Top Wall boundary.

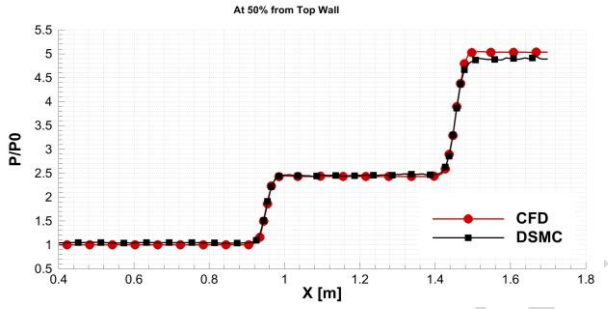

Fig. 5. Comparison of Pressure Ratio between CFD and DSMC results at the 50% distance from the Top Wall

4 RESULTS AND DISCUSSIONS

In this section, the effect of rarefaction is studied. As mentioned in the Physical

Specifications section, six cases with different levels of rarefaction are selected for investigation.

Figure 6 represents and compares the Mach number contours of all cases. It can be seen that as the level of rarefaction increases, the shape of the first oblique shock changes and thickens. The variation in shockwave thickness is not limited to the first oblique shock; the reflection also changes similarly. These changes in the structure of shock reflection are due to the increase in molecular mean free path. In other words, when density decreases, molecular collisions decrease, delaying the progress of shock wave creation and, subsequently, reflection. Furthermore, it can be observed that the minimum Mach number decreases with increasing rarefaction. This indicates that more rarefaction in the flow results in stronger shockwaves. The first theory is that, as the flow spends more time in the shock region, dissipating effects act more on the flow momentum, resulting in greater energy loss. Alternatively, the second theory suggests that, as the number of molecules diminishes with rarefaction, the effect of shockwaves applies to fewer molecules, causing a greater reduction in momentum. In other words, their inertia regarding momentum changes when passing through the shockwave decreases with reduced density. Moreover, considering the pressure and temperature distribution for three benchmark cases of 1.0×10^{-5}, 1.0×10^{-6}, and 0.25×10^{-6} in Figures 7 and 8, the increase in shockwave thickness is evident. Figures 7 and 8 are drawn for each case at six different distance fractions from the upper wall, along straight lines in the domain. Considering the upper section of each graph, from left (red line) to right (black line), the graph starts from the top wall and extends to distances of 90%, 80%, 70%, 50%, and 25% from the top wall, respectively. Analyzing both the P-X and T-X graphs, the thickness of shockwaves can be observed through the curvature of the line graphs. In the near-continuum case, the changes are sharp, and the sharpness of the lines represents this. In more rarefied cases, the graph lines bend and turn into curved lines, indicating a gradual change in properties. This gradual change means the shockwaves have thickened. Comparing different distances from the top wall shows that this change is uniform across all domain sections. Considering the pressure ratios and temperature ratios in four different rarefactions in Figures 9 and 10, the figures show that shockwave thickness does not affect wall transport phenomena.

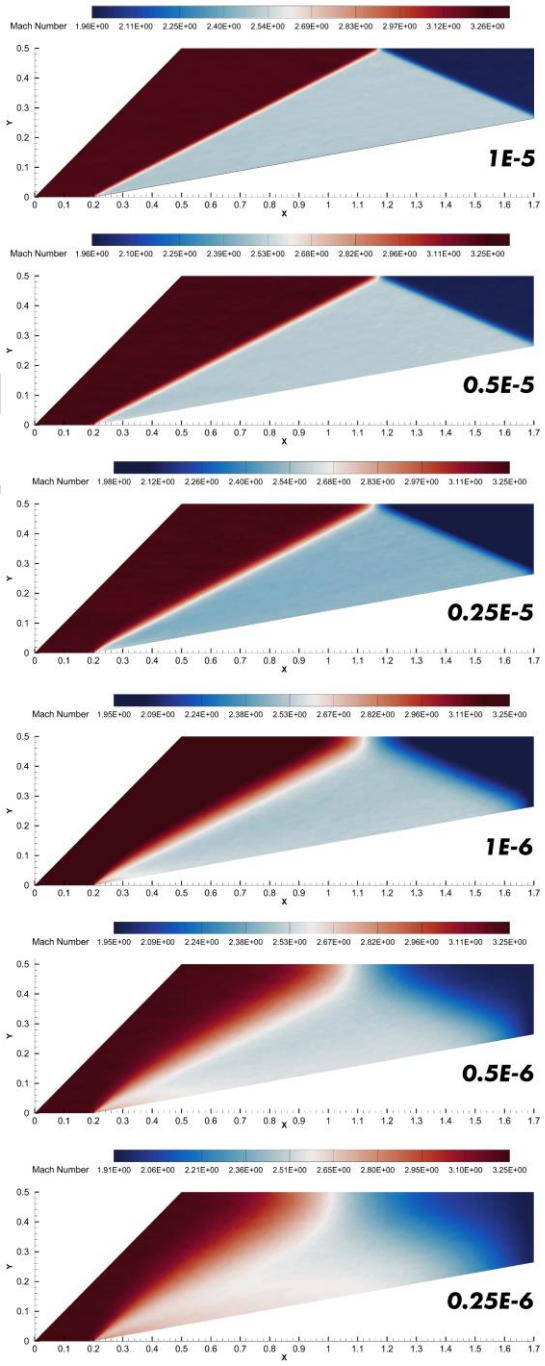

Fig. 6. Mach number contour for all cases

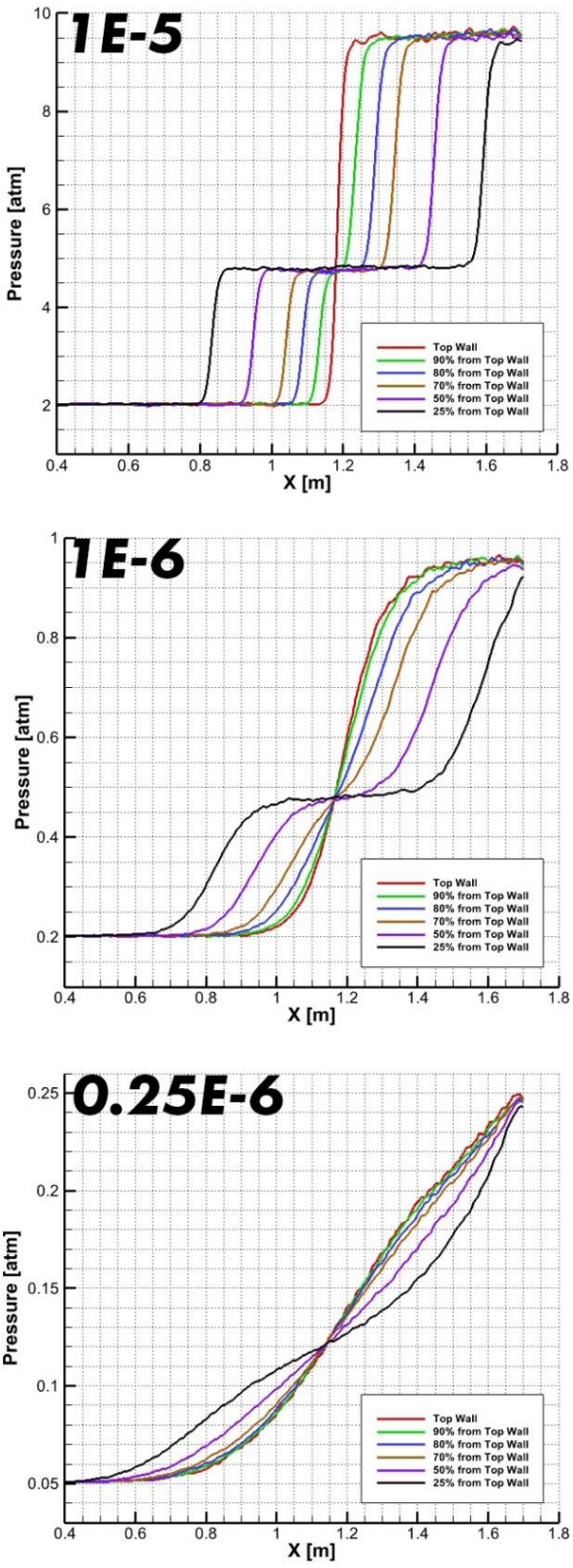

Fig. 7. Pressure and Temperature distribution at different distances from the top wall

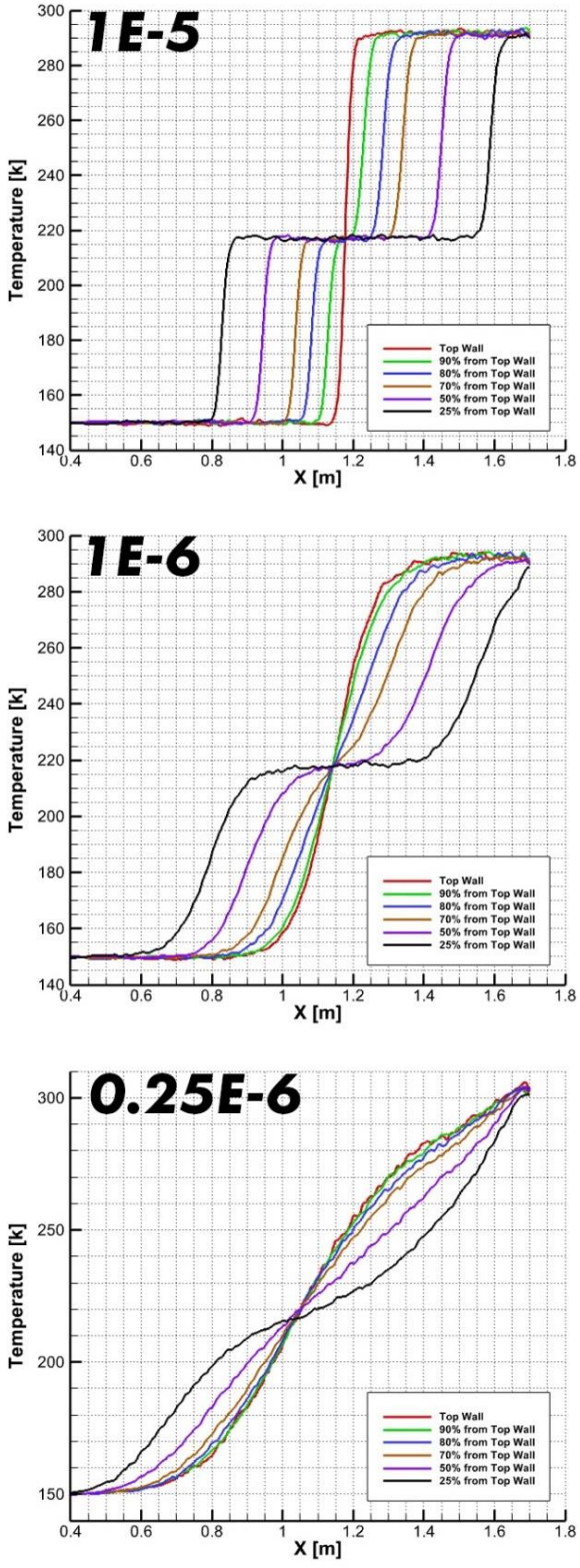

Fig. 8. Temperature distribution at different distances from the top wall

This means that the pressure and temperature on the top wall change in one step, but at a distance of 50% from the

top wall, it happens in two steps for the near-continuum case. Increasing rarefaction results in merging these steps into one step. This indicates that shockwaves are moving closer to each other due to their thickness. The key point here is that, in the most rarefied case of 0.25×10^{-6}, when both waves are merged, their behavior tends to resemble a normal shock. This is evident in the maximum temperature ratio in this case, which is considerably higher than in the rest of the cases.

Moreover, by defining a new concept named total shock thickness, which is the required distance to pave in the X direction to completely pass from the shockwave effects, a new comparison can be done. Considering Figure 8, the 25% line for the case of 1×10^{-5}, it can be observed that the first shockwave starts from 0.8 m, and an increase in temperature occurs, and ends at around 0.9 m, and the reflection starts at 1.55 m and ends at 1.65 m. By the new definition of total shock thickness, a thickness of 0.1 m is observed for the near continuum case. Now, compared to the 1×10^{-6}, by ten times more rarefaction, the total shock thickness increases to 0.5 m, which is 5 times the continuum case, and for the 0.25×10^{-6}, it's around 0.65 m, resulting from four times more rarefaction.

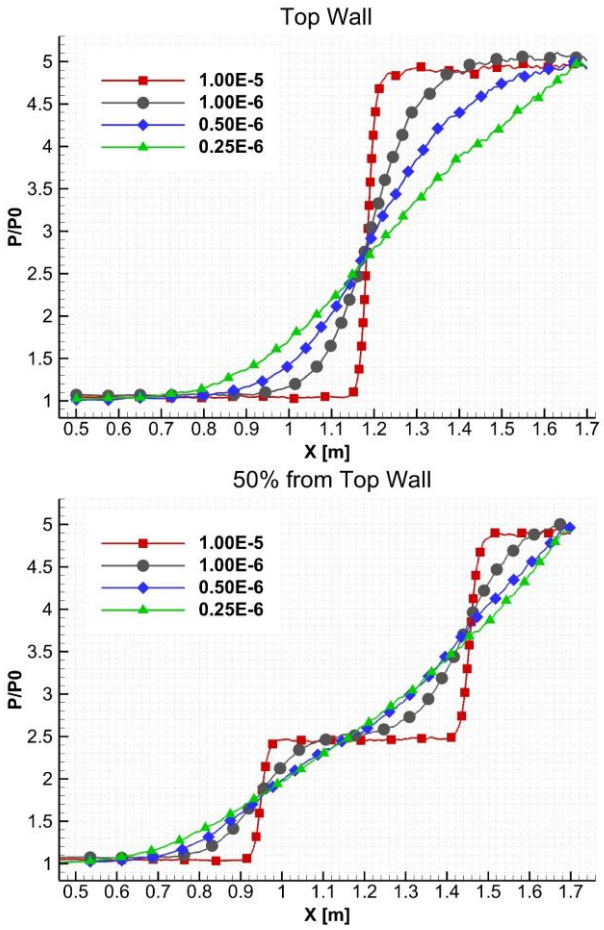

Fig. 9. Pressure ratio for different rarefaction levels at the top wall and 50% distance from the top wall

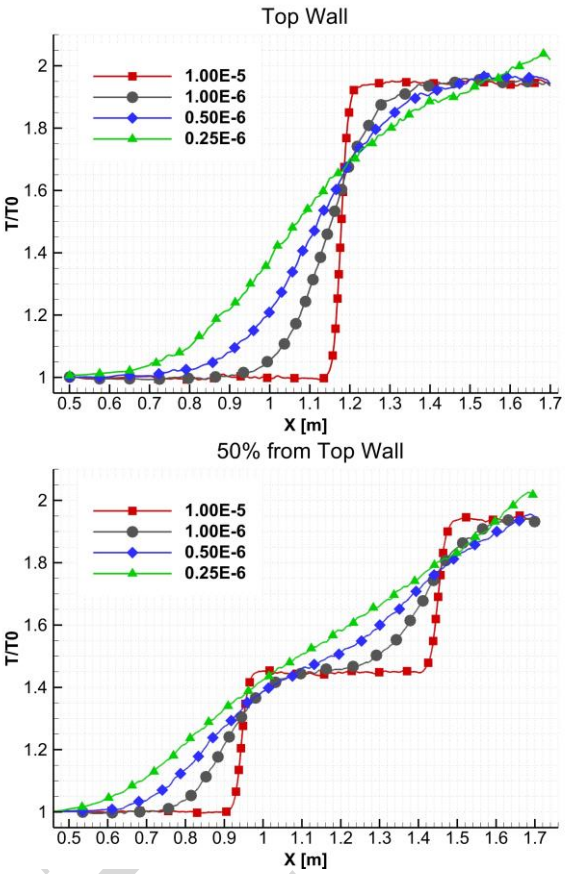

Fig. 10. Temperature ratio for different rarefaction levels at the top wall and 50% distance from the top wall

5 CONCLUSIONS

This study employed the Direct Simulation Monte Carlo (DSMC) method to investigate shock wave reflection behavior in supersonic rarefied gas flows within a channel featuring a ramp. The analysis demonstrated that increased flow rarefaction, characterized by higher Knudsen numbers, induces significant thickening of both incident and reflected shockwaves, with the reflected wave exhibiting a more pronounced sensitivity to rarefaction effects. Crucially, non-equilibrium regions near the shock origins lead to curved, thickened wave structures rather than sharp discontinuities, resulting in a progressive rather than instantaneous change in aerothermodynamic flow properties (pressure, temperature, velocity). This thickening phenomenon was quantitatively observed to increase substantially with the degree of rarefaction. Furthermore, heightened rarefaction was found to enhance shock strength, as evidenced by lower post-shock Mach numbers and elevated maximum temperature ratios, potentially

attributable to extended dissipation timescales within the thickened shock structure or reduced molecular inertia at lower densities. In highly rarefied regimes, the thickening causes the incident and reflected shock structures to merge spatially, exhibiting characteristics akin to a normal shock. While rarefaction significantly alters the internal shock structure and wave merging, its direct impact on near-wall pressure and temperature transport was found to be comparatively limited. This work establishes a foundational understanding of rarefied shock reflection dynamics, providing critical insights relevant to high-speed aerodynamics and vacuum system design. Future research should extend this investigation to examine shockwave interactions with solid structures in rarefied flows, a crucial consideration for applications such as reentry vehicle aerothermodynamics.

CONFLICT OF INTEREST

The authors declare that they have no conflict of interest.

REFERENCES

[1] G. Bird, "Shock wave: Boundary Layer interactions in rarefied gas flows," in *26th Thermophysics Conference*, Honolulu, HI, U.S.A., 2012, Paper AIAA-91-1312-CP, https://doi.org/10.2514/6.1991-1312.

[2] R. Nance, H. Hassan, B. Hollis, and T. Horvath, "Solution of transitional wake flows at Mach 10," in *7th AIAA/ASME Joint Thermophysics and Heat Transfer Conference*, 1998, Paper 2939, https://doi.org/10.2514/6.1998-2939.

[3] V. Titarev, A. Frolova, and E. Shakhov, "Rarefied Gas flow reflection from a wall with an orifice and gas outflow into a vacuum," *Fluid Dynamics*, vol. 54, no. 4, pp. 550-557, 2019, https://doi.org/10.1134/S0015462819040104.

[4] H. Akhlaghi, E. Roohi, A. Daliri, and M. R. Soltani, "Shock polar investigation in supersonic rarefied gas flows over a circular cylinder," *Physics of Fluids*, vol. 33, no. 5, 2021, https://doi.org/10.1063/5.0050571.

[5] S. Takata, K. Aoki, and C. Cercignani, "The velocity distribution function in an infinitely strong shock wave," *Physics of Fluids*, vol. 12, no. 8, pp. 2116-2127, 2000, https://doi.org/10.1063/1.870457.

[6] T. Holtz and E. Muntz, "Molecular velocity distribution functions in an argon normal shock wave at Mach number 7," *The Physics of fluids*, vol. 26, no. 9, pp. 2425-2436, 1983, https://doi.org/10.1063/1.864428.

[7] G. Zuppardi and C. Boffa, "Effects of rarefaction on the shock wave/boundary layer interaction in hypersonic regime," in *AIP Conference Proceedings*, 2012, vol. 1501, no. 1, pp. 673-679: American Institute of Physics, https://doi.org/10.1063/1.4769607.

[8] S. T. Gardner and R. K. Agarwal, "Effects of rarefaction and thermal non-equilibrium on a blunt body and a bicone in hypersonic flow and their shape optimization for reducing both drag and heat transfer," in *AIP Conference Proceedings*, 2019, vol. 2132, no. 1, Paper 100010: AIP Publishing LLC, https://doi.org/10.1063/1.5119605.

[9] H. Akhlaghi, R. Shafiei, and A.-R. Rahmati, "A wall-function viscosity model based on gas molecular dynamic simulation and its application," *International Journal of Modern Physics C*, 2025, Art. no. 2550115, https://doi.org/10.1142/S0129183125501153.

[10] E. Roohi, H. Akhlaghi, and S. Stefanov, *Airfoil Aerodynamics at Rarefied Flow Regimes*, in *Advances in Direct Simulation Monte Carlo: From Micro-Scale to Rarefied Flow Phenomena*. 2025, Springer Nature Singapore: Singapore. pp. 409–442.

[11] Y. Jiang and T. Ma, "Investigation of shock-shock interaction in hypersonic rarefied flow using direct simulation Monte Carlo method," *ArXiv Preprint ArXiv:2410.00351*, 2024, https://doi.org/10.48550/arXiv.2410.00351.

[12] H. Akhlaghi, E. Roohi, and S. Stefanov, "On the consequences of successively repeated collisions in no-time-counter collision scheme in DSMC," *Computers and Fluids*, vol. 161, pp. 23-32, 2018, https://doi.org/10.1016/j.compfluid.2017.11.005.